Supplementary Appendix

This appendix has been provided by the authors to give readers additional information about their work.

Supplement to: Hara Y, Balci-Hayta B, Yoshida-Moriguchi T, et al. A dystroglycan mutation associated with limb-girdle muscular dystrophy. N Engl J Med 2011;364:939-46.

SUPPLEMENTARY METHODS

Additional clinical information

Clinical data on this patient were reported previously[14]. Briefly, the onset of disease occurred at approximately three years of age, shortly after the patient started to walk. Her initial difficulties were an unsteady gait and difficulty climbing stairs. She has mild calf enlargement and ankle contractures, as well as increased lumbar lordosis. The patient was independently ambulant, but only for short distances (25-30 meters) at 16 years of age. Her intellectual development has been slow: she said her first few words at 7 years of age, and she used only two-word sentences at 16 years of age. At age 16 her IQ was 50, and she was unable to count money and perform independent activities. The creatine kinase concentration at the age of 15 was 4133 U/L. Her cranial MRI was normal.

Cell culture

The dystroglycan$^{-/-}$ myoblast cell line was established as previously described[26]. Briefly, Dystroglycan$^{flox/flox}$ mice were crossed with H-2Kb-tsA58 transgenic mice[26,27], and limb muscles from E18.5 dystroglycan$^{flox/flox}$; H-2Kb-tsA58 embryos were dissociated with 0.2% trypsin and 0.01% DNase. Cells were resuspended in growth medium (DMEM, 1 mM glutamine, 4.5 mg/ml glucose, 10% FBS, 10% horse serum, 0.5% chick embryo extract (Sera Laboratories Inc.), and gentamycin), supplemented with 20 U/ml of recombinant mouse interferon-γ (Sigma-Aldrich, I4777, St. Louis, MO) and pre-plated for 20 min at 33°C. Non-adherent cells were transferred to a Matrigel-coated tissue culture dish (BD Falcon, San Jose, CA) and maintained in growth medium at 33°C/10% CO_2. Dystroglycan$^{flox/flox}$ myoblasts that had been screened for their ability to differentiate into myotubes were infected with a pBabe-Cre retroviral vector, and

dystroglycan$^{-/-}$ myoblasts were identified by PCR. TSA201, a transformed human kidney cell line stably expressing an SV40 T antigen, was cultured as previously described[15].

Antibodies

The monoclonal antibody to the glycosylated form of α-dystroglycan (IIH6), as well as the polyclonal antibody to β-dystroglycan (βDG; ap83), that were used had been characterized previously[3]. The CORE antibody (sheep5, against the α-dystroglycan core protein) is from sheep antiserum raised against the whole dystrophin-glycoprotein complex and had also been characterized previously[3]. Anti-laminin (L9393), and anti-myc tag (clone 4A6) antibodies were purchased from Sigma-Aldrich (St. Louis, MO), and Millipore (Billerica, MA), respectively. Biotinylated anti-human IgG was obtained from Vector Laboratories (Burlingame, CA). An antibody against the Laminin α1 chain (clone 317) was a kind gift from Dr. Lydia Sorokin (Münster University, Münster, Germany).

Vector construction

The T192M-dystroglycan mutation was introduced into expression vectors encoding rabbit dystroglycan, using a conventional PCR method. To generate adenoviral vectors expressing the T192M-dystroglycan mutant, we subcloned a full-length cDNA carrying the T192M mutation into the HindIII and NotI sites of the vector pAd5RSVK-NpA (obtained from the University of Iowa Gene Transfer Vector Core). Adenoviral vectors were generated as described elsewhere[15]. Construction of expression vectors encoding Fc2 (the dystroglycan N-terminus) or Fc5 (α-dystroglycan) were described elsewhere[15].

Biochemical and ligand-binding analyses

Glycoprotein enrichment and Western blotting were performed as described previously, with minor modifications[3,15].

For the cell-surface biotinylation assay, myoblasts infected by adenoviruses expressing WT- or T192M-dystroglycan were washed three times with ice-cold PBS (-) and incubated with PBS (-) containing the membrane impermeable sulfo-NHS-LC-biotin reagent (PIERCE, Rockford, IL) for one hour at 4°C. The cells were then washed twice at room temperature with PBS (-) containing 100 mM glycine, to quench the cross-linker and remove excess biotin. Cells were rinsed in PBS (-) and lysed in Buffer A (150 mM NaCl, 50 mM Tris, pH 7.5) plus 1% Triton X-100 containing a cocktail of protease inhibitors. Cell-surface proteins were immunoprecipitated from the biotin-labeled cells using ImmunoPure Immobilized Streptavidin (PIERCE, Rockford, IL). The samples were then analyzed by Western blotting with the IIH6, CORE, and βDG antibodies.

For the pull-down assay, fusion proteins encoding full-length α-dystroglycan and the α-dystroglycan N-terminus bearing the T192M mutation and attached to Fc (Fc5 and Fc2, respectively) were expressed independently in TSA201 cells and purified from the cell lysates using Protein-A affinity beads[15]. The affinity bead-DGFc fusion protein complexes were then incubated with lysates from TSA201 cells expressing myc-tagged LARGE[28]. Materials bound to the beads were eluted with Laemmli sample buffer and analyzed by Western blotting. Binding between dystroglycan and LARGE was detected using the Odyssey infrared imaging system (LI-COR Biosciences, Lincoln, NE).

Ligand overlay and laminin solid-phase assays were performed as previously described[3,15,29].

To analyze laminin clustering, dystroglycan-null myoblast cell-line was infected with adenoviral vectors, at an MOI of 1000, in growth medium. At 24 hours post-infection, cells were seeded onto 8-well glass slides (BD biosciences, San Jose, CA) coated with fibronectin (Sigma-Aldrich, St. Louis, MO). After an additional 24 hours of incubation, the culture medium was replaced with fresh medium containing 7.5 nM mouse EHS Laminin-I (Invitrogen, Carlsbad, CA) and the cells were incubated in this medium for 16 hrs. After fixation (4% paraformaldehyde) and blocking, the cells were

co-stained with the anti-Laminin α1 chain (clone No. 317) and CORE antibodies. Confocal microscopy was performed images were analyzed using FV10 ver-1.5 (Olympus, Center Valley, PA). Data show the mean ± s.e.m. for three independent experiments.

Generation of the T190M-dystroglycan knock-in mice

Genomic fragments of the mouse *Dag1* gene were isolated from a 129/Sv genomic library[30]. The nucleotide sequence encoding Thr-190 (GTC CTT ACA GTG ATT) was mutated to encode a methionine, and a CviAII restriction site was introduced simultaneously (sequence of the mutant allele: GTC CTC **ATG** GTG ATT; the methionine codon is shown in bold, and the CviAII site is underlined). The Neo cassette flanked by LoxP sites was inserted into a SalI site located between exon 2 and exon 3. A thymidine kinase cassette was attached to the 5' end of the vector for negative selection. The NotI-linearized construct was electroporated into R1 ES cells, and cell clones resistant to positive and negative selection were screened by PCR over the 5' and 3' sides of the insertion. Positive ES clones were microinjected into C57BL/6J blastocysts to generate chimeric mice. PCR-based genotyping of each locus was carried out using the following primers: 5'-homologous recombination: #5742 (5'-CGTCCGCCCCTTTCTGTTCTGGTTACTC -3') and #5737 (5'-GCGGGGCTGCTAAAGCGCATGCTCCAGA -3'); 3'- homologous recombination: #5856 (5'-CATCGCCTTCTATCGCCTTCTTGACGAGTT -3') and #5857 (5'-CTCTTCTGAGGCACATCTCCCATCACG -3'). To confirm that the T190M mutation was present in the *Dag1* locus, we amplified the mutation-containing DNA fragment (426 bp) using the following primers: #5530 (5'-TGATGGTAACATTTATAACTCACAC-3') and #5531 (5'-GTTGTGAAGTTCTACTTCTGAGAAGCTC-3'). The resultant fragment was digested with CviAII (New England Labs, Ipswich, MA), yielding bands of 327 and 99 bp from the T190M-encoding allele.

Analysis of the T190M-dystroglycan knock-in mice

Immunofluorescence analysis and hematoxylin-eosin staining were carried out as described previously[3]. For the fore-limb grip-strength test, T190M (n=10) and littermate control (WT; n=9) mice at 11-20 weeks of age were examined using a grip-strength meter (Columbus Instruments, Columbus, OH, model #1027). This test was repeated five consecutive times within the same session, and the means of all trials were recorded. For analysis of NMJs with Alexa488-labelled α-bungarotoxin, diaphragm sections (30-40 μm) or whole diaphragm samples were prepared from adult T190M knock-in mice or their littermate controls. Those samples were fixed with 4% paraformaldehyde in PBS (sections: for 20 min; whole diaphragm: for three hours), and permeabilized with 0.5% Triton X-100 in PBS for 10 min on ice. After blocking with 3% BSA in PBS, the sections were incubated with Alexa488-labeled α-bungarotoxin (Invitrogen, Carlsbad, CA) overnight at 4°C. Images were taken using a confocal microscope (FV10 ver-1.5, Olympus, Center Valley, PA), and analyzed using the Image Pro plus program (Media Cybernetics, Bethesda, MD). For Evan's blue dye (EBD) uptake assay, adult T190M knock-in mice and littermate controls were injected with EBD one day before exercise. Those mice were subjected to downhill running on a treadmill with a built-in shock grid at a 15 degree declination. After a warm-up running (3 m/min, 5 minutes), the initial running speed of 10 m/min was increased every 5 minutes by 5 m/min until the maximal speed (25 m/min) was reached. Exhaustion was defined as the point at which the animal would not resume running. Tissues were harvested at one day after the exercise. In evaluating cardiac muscle pathology, we used skeletal and cardiac muscle-specific (*MCK*-cre) dystrolgycan-deficient mice[27] as a control. HFaq treatment and an IMAC bead binding assay were performed as described previously[12]. Rotarod performance was tested in T190M knock-in mice and littermates, 10 to 15 weeks of age, using the ROTOR-ROD system (San Diego Instruments, San Diego, CA). The mice were placed on top of the beam, and the rotarod accelerated gradually, without jerks, from 0 to 35 rpm

over a two-minute trial. Latencies for the mice to fall from the rod were recorded automatically. Each mouse was subjected to 5 trials at 15-min intertrial intervals, on each of three consecutive days.

Molecular modeling

The N-terminal portion of the T192M mutant of α-dystroglycan was modeled using the SWISS-MODEL program for the analysis, and the crystal structure of the WT mouse orthologue as a template (Ref. 23, PDB accession No. 1u2c). The figure was prepared using the program PyMOL v-0.99 (DeLano, W.L. The PyMOL Molecular Graphics System (2002) DeLano Scientific, San Carlos, CA, http://www.pymol.org).

Author contributions

Y.H., P.D. and K.P.C. designed the study. B.B., H.G., B.T., F.M., H.T. and P.D. diagnosed patients, collected blood from the patient, and analyzed genetic data. S.J.B. provided the dystroglycan-null myoblast cell line from our skeletal muscle-specific conditional knockout mice. Y.H. and M.K. performed biochemical studies, with the assistance of T.Y.-M., T.W., S.K. and M.B.A.O. D.B., T.Y.-M., T.W., J.S.S., S.K., M.B.A.O. and F.M. provided critical discussion on the research. Y.H. and R.W.C. performed the mouse studies. Y.H. and A.A. performed the structural modeling studies. K.P.C supervised and mentored all work. Y.H. and K.P.C. wrote the initial manuscript, and all authors contributed to the final version of the manuscript.

SUPPLEMENTARY REFERENCES

26. Herbst R, Burden SJ. The juxtamembrane region of MuSK has a critical role in agrin-mediated signaling. Embo J 2000;19:67-77.

27. Cohn RD, Henry MD, Michele DE, et al. Disruption of *Dag1* in differentiated skeletal muscle reveals a role for dystroglycan in muscle regeneration. Cell 2002;110:639-48.

28. Rojek JM, Campbell KP, Oldstone MB, Kunz S. Old World arenavirus infection interferes with the expression of functional alpha-dystroglycan in the host cell. Mol Biol Cell 2007;18:4493-507.

29. Sugita S, Saito F, Tang J, Satz J, Campbell K, Sudhof TC. A stoichiometric complex of neurexins and dystroglycan in brain. J Cell Biol 2001;154:435-45.

30. Williamson RA, Henry MD, Daniels KJ, et al. Dystroglycan is essential for early embryonic development: disruption of Reichert's membrane in *Dag1*-null mice. Hum Mol Genet 1997;6:831-41.

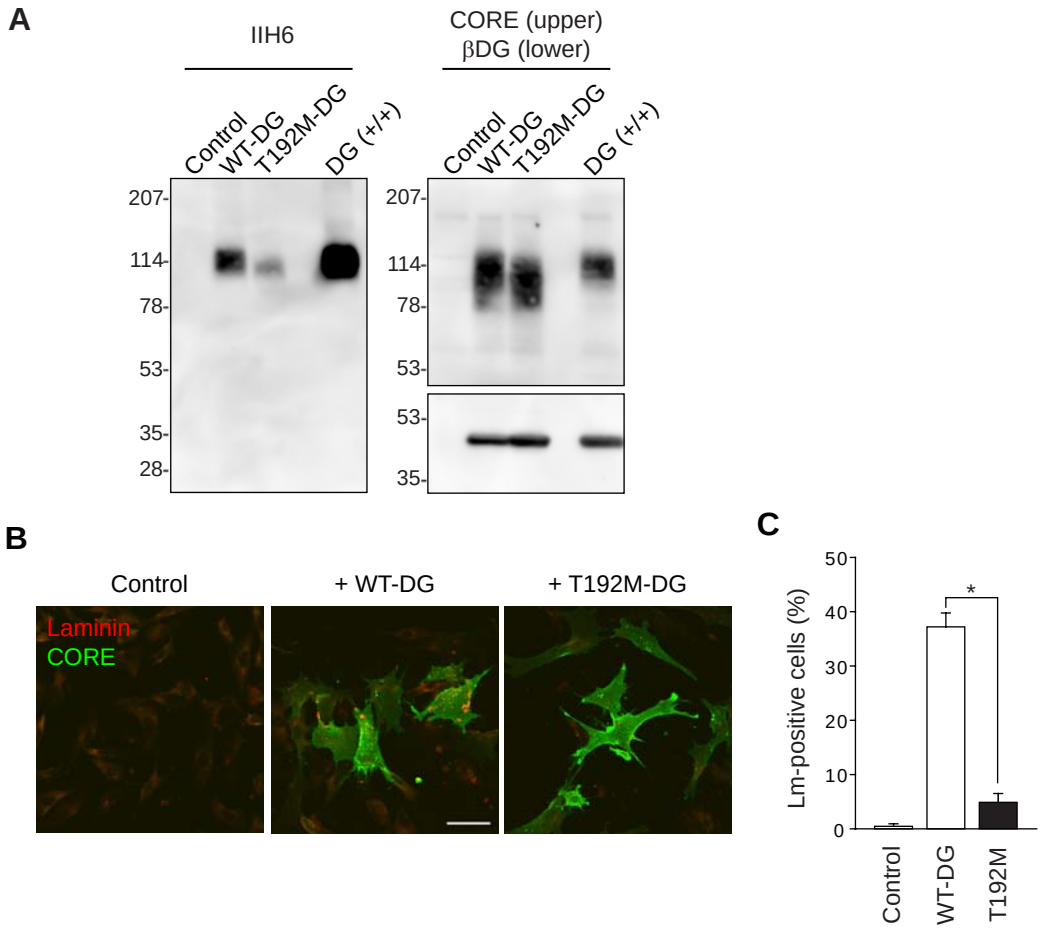

Supplementary Figure 1 | Biochemical analyses of the WT- and T192M-dystroglycan proteins in dystroglycan-null myoblast cells.

Panel A shows cell-surface expression of the WT- and T192M-dystroglycan proteins in dystroglycan-null myoblast cells. WT- and T192M-dystroglycan-expressing cells were incubated with EZ-link Sulfo-NHS-LC-biotin. After membrane solubilization, biotinylated proteins were enriched using streptavidin-immobilized beads and subjected to Western blotting with the IIH6, CORE, and βDG antibodies. Panel B shows organization of laminin on the cell surface, in WT- and T192M-dystroglycan-expressing myoblast cells. Laminin clustering was observed only on cells expressing adenovirus-encoded WT-DG. The cells were co-stained with anti-laminin (clone #317) and CORE antibodies. White bar: 50 μm. Panel C shows statistical analysis of laminin clustering activity on WT- (open column) and T192M- (filled column) dystroglycan. Asterisk, $P<0.001$ (Student's *t*-test).

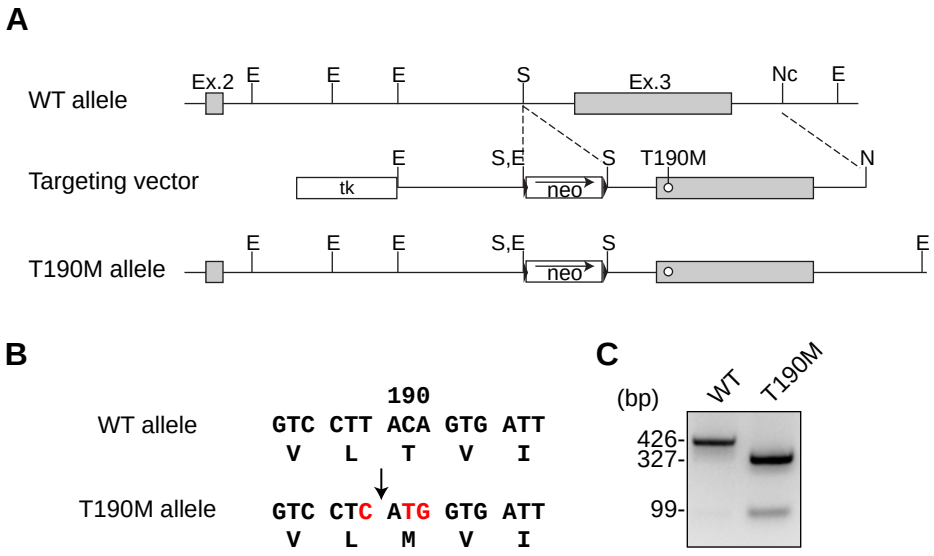

Supplementary Figure 2 | Generation of a mouse model harboring the T190M mutation.

Panel A shows a schematic representation of the WT *Dag1* allele, the targeting vector, and the homologously recombined allele. The open circle in exon 3 indicates T190M, which corresponds to the human T192M mutation. The thymidine kinase and Neo cassettes are illustrated as boxed tk and Neo, respectively. Filled arrowheads flanking the Neo cassette indicate loxP sites. Selected restriction enzyme cleavage sites are indicated above the gene (E: EcoRI; N: NotI; Nc: NciI; and S: SalI). Panel B shows engineered sequence abnormalities in the T190M knock-in mice, with nucleotide sequence shown at top and amino acid sequence shown at bottom. The knock-in sequence includes a recognition site for the restriction enzyme CviAII (marked by arrow). Panel C shows representive PCR genotyping analysis of the T190M-homozygous (T190M) mice. PCR products containing the T190M mutation are cleaved by CviAII.

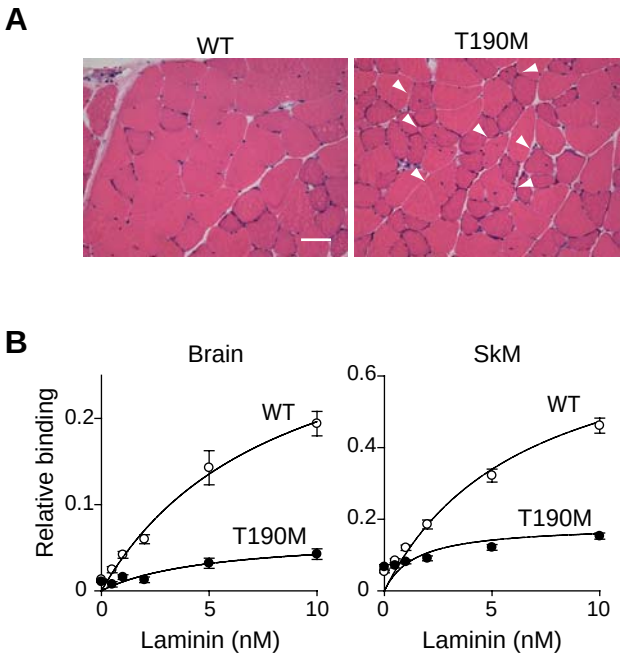

Supplementary Figure 3 | Further histological and biochemical analyses of a mouse model harboring the T190M mutation.

Panel A shows H&E-stained sections of gastrocnemius muscle, revealing the presence of centrally located nuclei in this muscle in the T190M mouse at 21 weeks of age. White arrowheads denote pathologic fibers. White bar: 50 μm. Panel B summarizes the results of solid-phase laminin-binding assays with WGA homogenates of brain (left) and skeletal muscle (right) from T190M mice and their littermate controls.

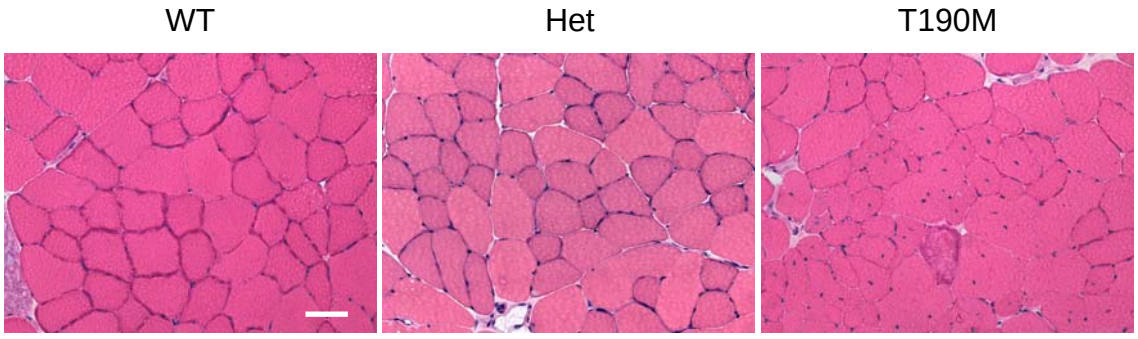

Supplementary Figure 4 | Histological analysis of one-year-old T190M mice.

H&E staining of wild-type (WT), heterozygous (Het), and T190M iliopsoas muscle taken from one-year-old mice. Myofibers with centrally localized nuclei were only observed in the homozygous mouse. Scale bar: 50 μm.

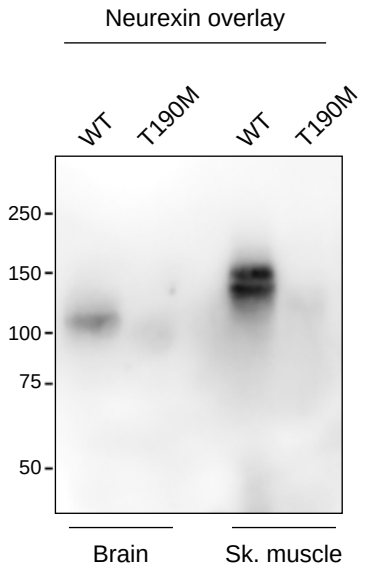

Supplementary Figure 5 | Neurexin overlay assay with WT- and T190M-dystroglycan

Representative image of neurexin overlay assay with WT- and T190M-dystroglycan. The membrane of WGA-enriched fractions prepared from WT and T190M mice were subject to the ligand overlay assay, using neurexin-immunoglobulin fusion protein[3,29]. Neurexin binding activity was significantly reduced on T190M-dystroglycan.

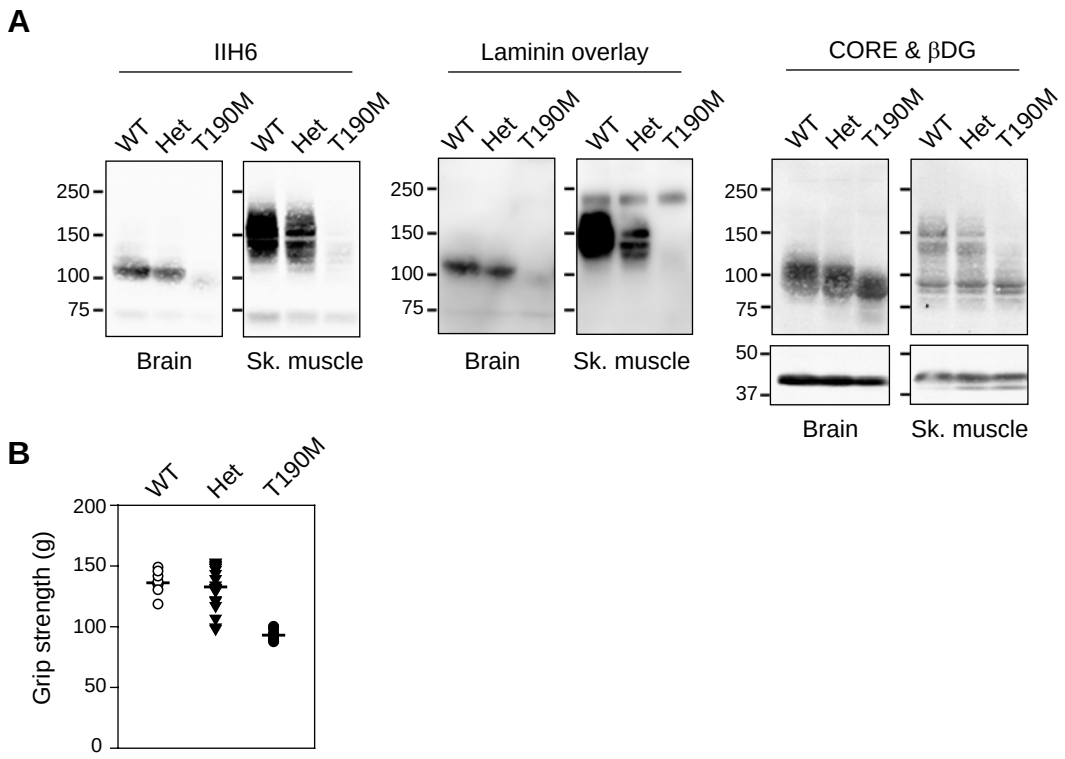

Supplementary Figure 6 | Phenotypic analysis of T190M heterozygous mice

Panel A shows representative images of Western blot analysis of WT, Het, and T190M mice. Expression and glycosylation of dystroglycan were evaluated using the IIH6 antibody (left), Laminin overlay (middle), and CORE & βDG antibodies (right). Panel B displays results from the grip strength test among WT, Het, and T190M mice. Reduction in grip strength was observed in T190M mice compared with WT and Het mice ($P<0.001$, One-way ANOVA test), but there was no statistical difference between WT and Het mice.

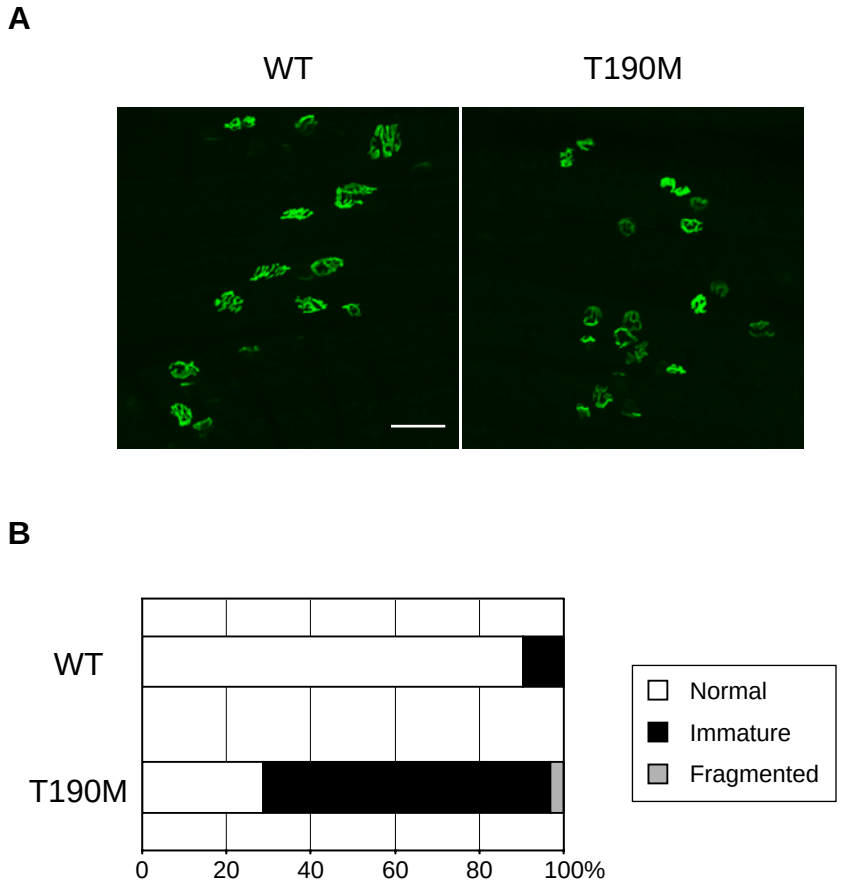

Supplementary Figure 7 | Morphological analysis of NMJs in WT and T190M diaphragm.

Panel A shows representative images of NMJs in WT and T190M muscle samples stained with Alexa488-labeled α-bungarotoxin. Scale bar: 50 μm. Note that NMJs in T190M diaphragms tend to be smaller and structurally less complex than those in WT diaphragms. Panel B shows evaluation of NMJ morphology in WT and T190M homozygous mice at the ages of 9-21 weeks old (Diaphragm, n = 218 for WT and n = 366 for T190M homozygous mice).

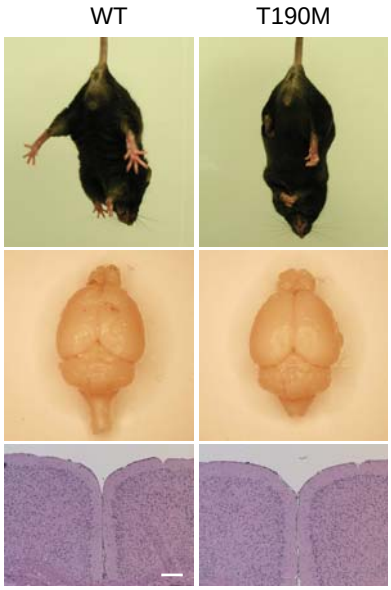

Supplementary Figure 8 | The T190M mouse model displays neurological phenotypes.

Top panels show representative WT (left) and T190M (right) mice suspended by the tail. Only mutant mice displayed a clasping phenotype (T190M: 13 out of 19 mice). Middle panels show gross structures of the control and T190M mutant brains. No structural abnormality was evident in the mutant mice. Bottom panels show histological sections of cerebral cortices of WT and T190M mice. H&E staining of the brain sections reveals that neuronal migration in the T190M brain was normal. White bar: 200 μm.

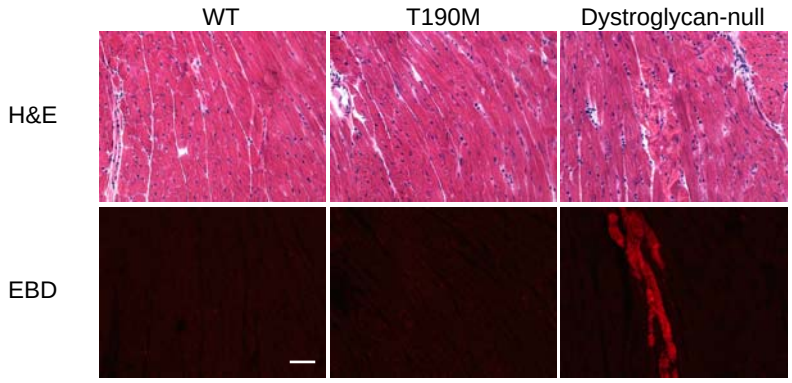

Supplementary Figure 9 | The T190M mutation does not affect cardiac muscle pathology in response to exercise stress in mouse.

Upper panels show H&E staining of cardiac sections from WT and T190M mice. Lower panels show Evans blue dye uptake (EBD, in Red) in the heart. Dystroglycan-null hearts were analyzed as negative controls[27]. EBD uptake was observed only in the dystroglycan-null hearts, suggesting that a deficiency in dystroglycan function causes susceptibility to exercise-induced cardiac membrane damage. White bar: 50 μm.

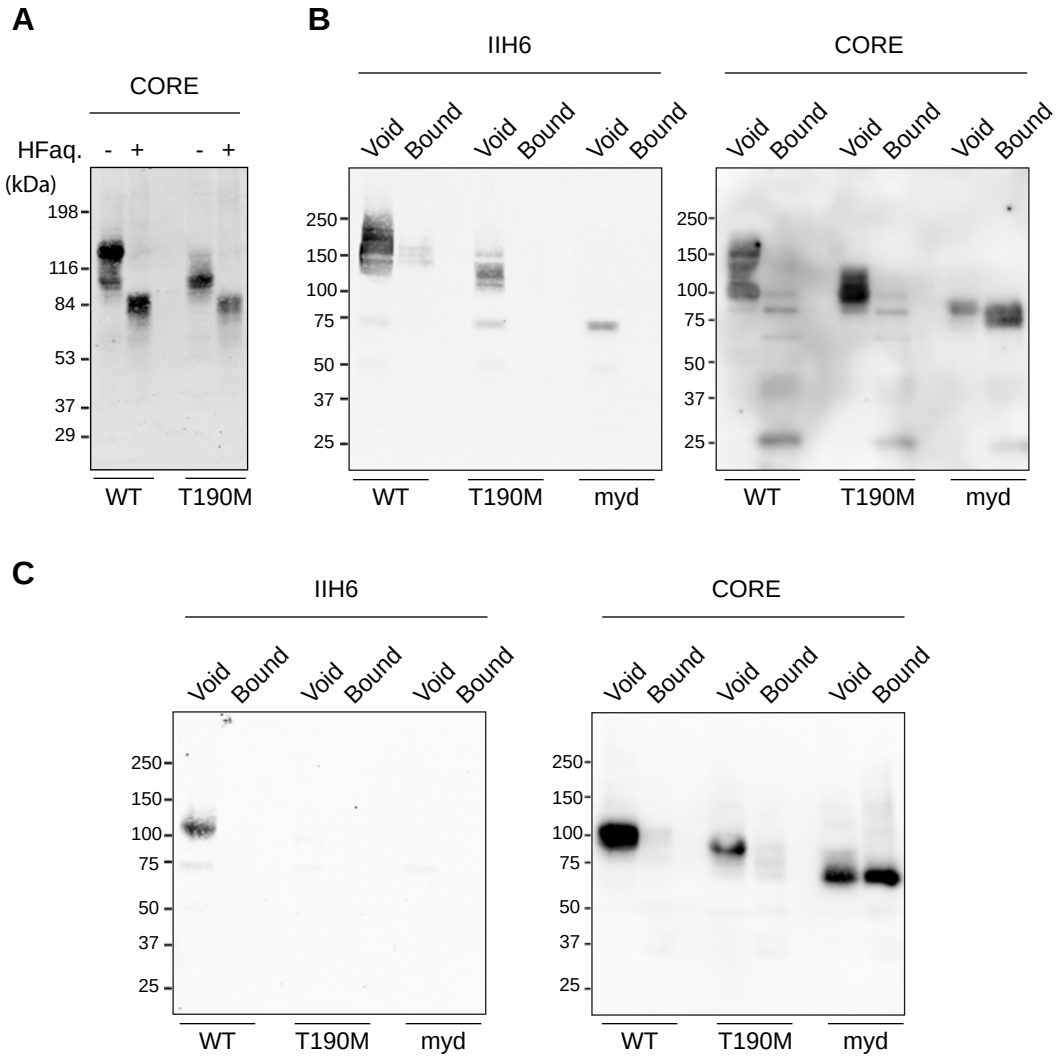
A
CORE
HFaq. - + - +
(kDa)
198
116
84
53
37
29
WT
T190M
B
IIH6
CORE
Void
Bound
250
150
100
75
50
37
25
WT
T190M
myd
C
IIH6
CORE
Void
Bound
250
150
100
75
50
37
25
WT
T190M
myd

Supplementary Figure 10 | The T190M mutation impairs maturation of dystroglycan's post-phosphoryl glycans.

Panel A shows the consequences of chemical dephosphorylation of α-dystroglycan by treatment with aqueous hydrofluoric acid (HFaq). WGA-enriched protein fractions of WT and T190M skeletal muscle were subject to HFaq treatment, which specifically cleaves phosphoester linkages. α-dystroglycan was detected using the CORE antibody. The observed reduction in the molecular weight of T190M α-dystroglycan following HFaq treatment indicates that further modification occurs on the α-dystroglycan phosphate residues in the muscle of these animals. Panels B and C show binding of α-dystroglycan to Immobilized Metal Affinity Chromatography (IMAC) beads. Glycoproteins from WT, T190M, and *Large*^{myd} (myd) muscle (Panel B) and brain (Panel C) samples were applied to IMAC beads. Bound and void fractions were analyzed by Western blotting with the IIH6 and CORE antibodies. Neither WT nor T190M α-dystroglycan bound to the beads, whereas myd α-dystroglycan was captured by the beads.

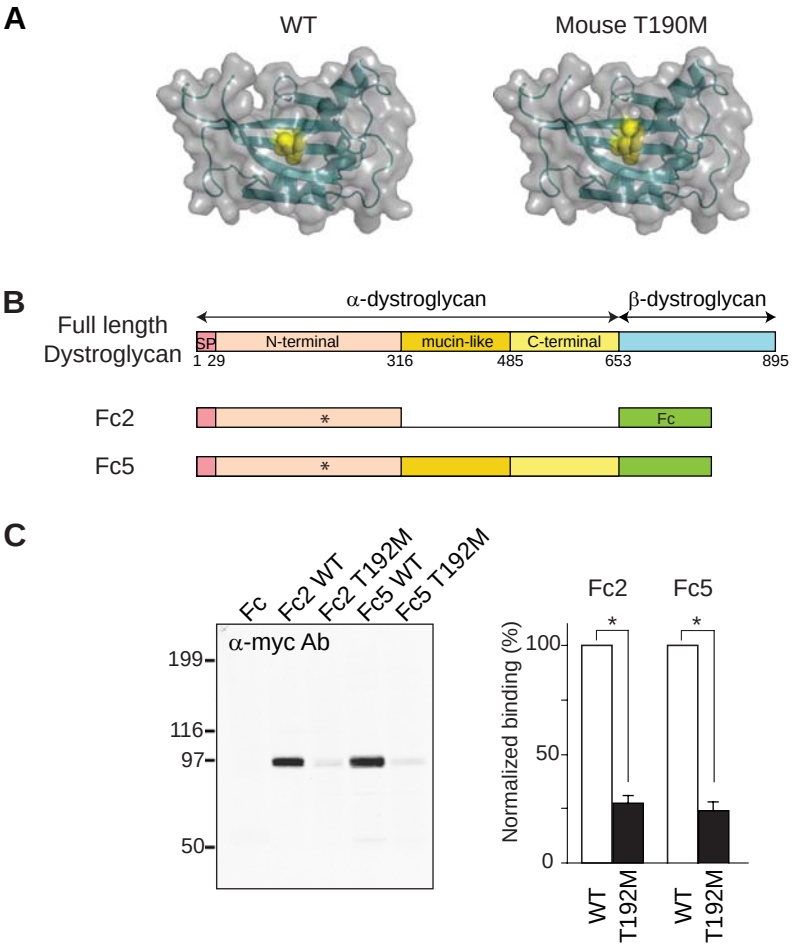
A
WT
Mouse T190M
B
Full length
Dystroglycan
α-dystroglycan
β-dystroglycan
SP
N-terminal
mucin-like
C-terminal
1 29
316
485
653
895
Fc2
Fc5
*
Fc
C
Fc
Fc2 WT
Fc2 T192M
Fc5 WT
Fc5 T192M
α-myc Ab
199
116
97
50
Fc2
Fc5
Normalized binding (%)
100
50
0
WT
T192M
WT
T192M

Supplementary Figure 11 | The T192M mutation disrupts the molecular interaction between dystroglycan and LARGE.

Panel A shows models of the RNA binding protein-like domain of the mouse dystroglycan N-terminus, based on the crystal structure of the WT dystroglycan N-terminus[23]. The model of the WT protein is shown on the left, and an *in silico* model of the mouse T190M mutant is shown on the right. Thr-190 and the mutated residues are indicated in yellow. The domain is displayed in surface representation, with ribbon diagrams superimposed (cyan). The crystal structure of the WT mouse dystroglycan N-terminus shows that Thr-190 is located in the middle of a cleft, with its side chain exposed[23]. In the *in-silico* model of the mouse T190M mutant protein, the overall fold is conserved but the bulky methionine side chain protrudes into the cleft, partially occluding it. Panel B shows a schematic representation of the α-dystroglycan:Fc fusion proteins. Fc5 (α-dystroglycan-Fc) and Fc2 (the dystroglycan N-terminus-Fc) were used for pull-down assays with LARGE. The position of residue Thr-192 is indicated by an asterisk. Panel C demonstrates that the dystroglycan N-terminus interacts molecularly with LARGE. (Left) A representative result from the pull-down assay, carried out with myc-tagged LARGE and an anti-myc antibody. (Right) Quantification of LARGE-binding activity by WT (open columns) and mutant (T192M, filled columns) dystroglycan-Fc proteins. Asterisk, $P<0.001$ (Student's *t*-test).